

PRIMORDIAL MAGNETIC FIELD AND NON-GAUSSIANITY OF THE 1-YEAR WILKINSON MICROWAVE ANISOTROPY PROBE (WMAP) DATA

PAVEL D. NASELSKY¹, LUNG-YIH CHIANG¹, POUL OLESEN¹, OLEG V. VERKHODANOV²
 naselsky@nbi.dk

Subject headings: cosmology: cosmic microwave background — cosmology: observations — methods: data analysis

Submitted to The Astrophysical Journal

ABSTRACT

Alfven turbulence caused by statistically isotropic and homogeneous primordial magnetic field induces correlations in the cosmic microwave background anisotropies. The correlations are specifically between spherical harmonic modes $a_{\ell-1,m}$ and $a_{\ell+1,m}$. In this paper we approach this issue from phase analysis of the CMB maps derived from the WMAP data sets. Using circular statistics and return phase mapping we examine phase correlation of $\Delta\ell = 2$ for the primordial non-Gaussianity caused by the Alfven turbulence at the epoch of recombination. Our analyses show that such specific features from the power-law Alfven turbulence do not contribute significantly in the phases of the maps and could not be a source of primordial non-Gaussianity of the CMB.

1. INTRODUCTION

After the release of the 1-year WMAP data for analysis (Bennett et al. 2003a,b,c; Hinshaw et al. 2003a,b), one of the most exciting area of investigation is in the statistical characterization of the CMB signal. After the WMAP science team's report on the observational constraint on the quadratic non-Gaussianity of the anisotropy of the CMB (Komatsu et al. 2003), Chiang, Naselsky, Verkhodanov & Way (2003); Coles, Dineen, Earl & Wright (2004); Naselsky, Doroshkevich & Verkhodanov (2003, 2004); Vielva et al. (2004); Park (2004); Eriksen et al. (2004); Hansen et al. (2004); Larson & Wandelt (2004) have reported detections of non-Gaussianity by various methods for the CMB maps derived from the WMAP data. Unfortunately, the origin of such non-Gaussian features, detected by different methods, is still unknown. In Chiang, Naselsky, Verkhodanov & Way (2003); Naselsky, Doroshkevich & Verkhodanov (2003, 2004); Eriksen et al. (2004), they point out that the non-Gaussian features might come from the foregrounds, whereas Hansen et al. (2004) argue in favor of systematic effects. Moreover, different methods detect various properties of non-Gaussian features from localized peculiar spots (Vielva et al. 2004) to global north-south asymmetry in the WMAP signal and COBE map as well (Eriksen et al. 2004).

There is another point of view on the issue of the WMAP non-Gaussianity. It comes from the theory of turbulence in magnetohydrodynamics (MHD). Using the so-called extended self-similarity (ESS) method, Bershadskii & Sreenivasan (2003, 2004) point out that the statistical properties of angular increments $\delta T_r = T(\mathbf{R} + \mathbf{r}) - T(\mathbf{R})$, where \mathbf{r} is the vector connecting two pixels $\mathbf{R} + \mathbf{r}$ and \mathbf{R} of the map, have the following relation in MHD $\langle |\delta T_r|^p \rangle \sim r^{\xi_p}$ for high order moments $p = 4, 6, \dots, 12$. For those moments, the ESS is clearly detected both in the COBE and the WMAP data : $\langle |\delta T_r|^p \rangle \sim \langle \delta T_r^4 \rangle^{\xi_p}$ where

$\xi_p = \frac{p}{8} + 1 - (\frac{1}{2})^{\frac{p}{4}}$. Moreover, in Branderburg, Enqvist & Olesen (1999); Durrer, Kahnashvili & Yates (1998); Mack, Kahnashvili & Kosowsky (2002); Subramanian, Seshadri & Barrow (2002); Chen et al. (2004) it was shown that primordial magnetic field, one of the most significant relics from inflation, can generate vorticity of Alfven waves before and during the epoch of hydrogen recombination. It interacts with the CMB photons, producing non-adiabatic tail of the CMB anisotropy and polarization. Assuming statistical homogeneity and isotropy on primordial magnetic field, it is shown that such Alfven turbulence shall have non-Gaussian properties, because of quadratic dependence of the vorticity amplitude on the magnetic strength \mathbf{B} . Namely, such a magnetic field induces correlation between the $a_{\ell-1,m}$ and $a_{\ell+1,m}$ multipole coefficients of the CMB temperature anisotropy expansion by the spherical harmonics.

An intriguing issue then follows: has WMAP observed the cosmological Alfven turbulence? Recently this issue is discussed in Chen et al. (2004), which exploits the correlations between $a_{\ell-1,m}$ and $a_{\ell+1,m}$ of the CMB caused by the vorticity of Alfven waves in order to put constraints on the strength of the magnetic field: $|\mathbf{B}| < 15$ nG for the spectral power index $n = -5$, and $|\mathbf{B}| < 1.7$ nG for the spectral power index $n = -7$.

In this paper we discuss this issue from another aspect: could the detected non-Gaussianity from the WMAP data be related to the Alfven turbulence? The basic idea is that even if the Alfven turbulence is small in amplitude in the CMB signal, it shall manifest itself in the WMAP maps between the phases $\phi_{\ell-1,m}$ and $\phi_{\ell+1,m}$. Phase correlation between Fourier modes has been investigated in relation to large-scale structure formation of the universe (Scherer, Melott & Shandarin 1991; Chiang & Coles 2000; Chiang, Coles & Naselsky 2002) and also applied as a test on non-Gaussianity (Chiang, Naselsky & Coles 2002; Chiang, Naselsky, Verkhodanov & Way 2003; Coles, Dineen, Earl

¹ Niels Bohr Institute, Blegdamsvej 17, DK-2100 Copenhagen, Denmark

² Special Astrophysical Observatory, Nizhniy Arkhyz, Karachay-Cherkessia, 369167, Russia

& Wright 2004) based on the random phase hypothesis as a practical definition of Gaussian random fields (Bardeen et al. 1986; Bond & Efstathiou 1987). Naselsky, Novikov & Silk (2002) use neighboring phase correlations to extract extragalactic point sources.

Assuming that the CMB signal is composed of pure Gaussian signal and sub-dominant vorticity tail, we use circular statistics on phases for such a signal in order to place constraint on the power spectrum of Alfvén turbulence at each multipole number ℓ . We will show that circular statistics allow us to decrease contamination of the dominant (Gaussian) part of the signal in order to investigate possible contamination from the non-Gaussian sub-dominant part.

2. CIRCULAR STATISTICS OF THE ALFVEN TURBULENCE

For statistical characterization of temperature fluctuations on a sphere we express each signal (either CMB or foreground components) as a sum over spherical harmonics:

$$\Delta T(\theta, \varphi) = \sum_{\ell=0}^{\infty} \sum_{m=-\ell}^{\ell} |a_{\ell m}| e^{i\phi_{\ell m}} Y_{\ell m}(\theta, \varphi), \quad (1)$$

where $|a_{\ell m}|$ and $\phi_{\ell m}$ are the moduli and phases of the coefficients of the expansion.

Homogeneous and isotropic CMB Gaussian random fields (GRFs), as a result of the simplest inflation paradigm, possess Fourier modes whose real and imaginary parts are Gaussian and mutually independent. The statistical properties are then completely specified by its angular power spectrum C_{ℓ}^{cmb} ,

$$\langle a_{\ell m}^{cmb} (a_{\ell' m'}^{cmb})^* \rangle = C_{\ell}^{cmb} \delta_{\ell \ell'} \delta_{m m'}. \quad (2)$$

In other words, from the Central Limit Theorem their phases

$$\Psi_{\ell m}^{cmb} = \tan^{-1} \frac{\Im(a_{\ell m}^{cmb})}{\Re(a_{\ell m}^{cmb})} \quad (3)$$

are randomly and uniformly distributed at the range $[0, 2\pi]$. We hereafter denote with G as the pure Gaussian tail of the CMB signal. For the combined signal

$$a_{\ell m} = G_{\ell m} + V_{\ell m}, \quad (4)$$

where $G_{\ell m}$ is the Gaussian tail and $V_{\ell m}$ is the vortex tail. We can write down

$$a_{\ell m} = |a_{\ell m}| \exp(i\Psi_{\ell m}), \quad (5)$$

where

$$|a_{\ell m}|^2 = |G_{\ell m}|^2 + |V_{\ell m}|^2 + 2|G_{\ell m}||V_{\ell m}| \cos(\Psi_{\ell m}^G - \Psi_{\ell m}^V);$$

$$\tan \Psi_{\ell m} = \frac{|G_{\ell m}| \sin \Psi_{\ell m}^G + |V_{\ell m}| \sin \Psi_{\ell m}^V}{|G_{\ell m}| \cos \Psi_{\ell m}^G + |V_{\ell m}| \cos \Psi_{\ell m}^V} \quad (6)$$

and $\Psi_{\ell m}^G, \Psi_{\ell m}^V$ are the phases of Gaussian and vortex at the (ℓ, m) harmonics, respectively.

In Durrer, Kahnashvili & Yates (1998) (hereafter DKY) it is shown that for the CMB anisotropy produced by the Alfvén turbulence, the properties of the power spectrum and phases are different from the adiabatic modes, which corresponds to the Gaussian tail of the signal. Namely, for the power spectrum $C_{\ell}(m) = \langle a_{\ell m} a_{\ell m}^* \rangle$ and the auto-correlator $D_{\ell}(m) = \langle a_{\ell-1, m} a_{\ell+1, m}^* \rangle$ from DKY we get

$$C_{\ell}(m) = A \frac{\Gamma(-n-1)\Gamma(\ell + \frac{n}{2} + \frac{3}{2})}{\Gamma(-\frac{n}{2})^2 \Gamma(\ell - \frac{n}{2} + \frac{1}{2})} \times$$

$$D_{\ell}(m) = \frac{2A}{|n+1|} \frac{\Gamma(-n-1)\Gamma(\ell + \frac{n}{2} + \frac{3}{2})}{\Gamma(-\frac{n}{2})^2 \Gamma(\ell - \frac{n}{2} + \frac{1}{2})} (\ell-1)(\ell+2) \times$$

$$\left[\frac{(\ell+m+1)(\ell-m+1)(\ell+m)(\ell-m)}{(2\ell-1)(2\ell+1)^2(2\ell+3)} \right]^{\frac{1}{2}}, \quad (7)$$

where A is the normalization constant and $-7 \leq n \leq -1$ is the power spectral index of the Alfvén turbulence. Below we discuss the models with $n = -3, -5$ and -7 , for which the mean power spectrum over m direction in Eq.(7) are $\overline{C}_{\ell}, \overline{D}_{\ell} \propto \ell^{n+3}$. Note that the model of $n = -5$ corresponds to the power spectrum $\overline{C}_{\ell} \propto \ell^{-2}$, which at the multipole range of $5 < \ell < 20$ has the same feature as that of the CMB for adiabatic perturbation. For the model of $n = -7$, on the other hand, the power of vertex tail is $\overline{C}_{\ell} \propto \ell^{-4}$ and increase rapidly if $\ell \rightarrow 0$, which is typical for the diffuse extragalactic foregrounds. For $n = -3$ the vertex power $\overline{C}_{\ell} \sim \text{const}$ mimic the power of extragalactic point source component. Therefore, simple statistics based on the estimation of the \overline{D}_{ℓ} -th moment from the WMAP data is potentially misleading, because of possible contribution from such kind of foregrounds as sub-dominant components to the signal.

The method we propose in this paper is based on the statistical characterization: non-Gaussianity of the vortex part of the CMB signal and related with correlation of the phases of $(\ell-1, m), (\ell+1, m)$ harmonics. The correlation vanishes for pure Gaussian CMB signal, whereas it is significant for the vortex component. We therefore, introduce some specific functions of phases which minimize the contribution from non-correlated Gaussian signal and maximize the non-Gaussian tail of the phases. For this purpose we use trigonometric moment statistics to counter the circular nature of phases (Fisher (1993), see also Naselsky, Doroshkevich & Verkhodanov (2003)). Let us define the following trigonometric moments:

$$\mathbf{C}(\ell) = \frac{1}{\ell-1} \sum_{m=1}^{\ell-1} \cos(\Psi_{\ell-1, m} - \Psi_{\ell+1, m});$$

$$\mathbf{S}(\ell) = \frac{1}{\ell-1} \sum_{m=1}^{\ell-1} \sin(\Psi_{\ell-1, m} - \Psi_{\ell+1, m});$$

$$r^2(\ell) = \mathbf{C}^2(\ell) + \mathbf{S}^2(\ell);$$

$$R = \frac{1}{\ell_{\max} - \ell_{\min} + 1} \sum_{\ell_{\min}}^{\ell_{\max}} r(\ell), \quad (8)$$

The reason for such statistics is clear. Simple algebra leads to the following properties of the phases:

$$\cos(\Psi_{\ell-1, m} - \Psi_{\ell+1, m}) =$$

$$|g_{\ell-1, m}| |g_{\ell+1, m}| \cos(\Psi_{\ell-1, m}^G - \Psi_{\ell+1, m}^G)$$

$$+ |v_{\ell-1, m}| |v_{\ell+1, m}| \cos(\Psi_{\ell-1, m}^V - \Psi_{\ell+1, m}^V)$$

$$+ |g_{\ell-1, m}| |v_{\ell+1, m}| \cos(\Psi_{\ell-1, m}^G - \Psi_{\ell+1, m}^V)$$

$$+ |g_{\ell+1, m}| |v_{\ell-1, m}| \cos(\Psi_{\ell+1, m}^G - \Psi_{\ell-1, m}^V) \quad (9)$$

where $|g_{\ell m}| = |G_{\ell m}|/|a_{\ell m}|, |v_{\ell m}| = |V_{\ell m}|/|a_{\ell m}|$. As one can see from Eq.(9) the first term is proportional to

$D_\ell(m) = \langle a_{\ell-1,m} a_{\ell+1,m}^* \rangle$ moment for the pure Gaussian tail of the signal, which should be vanish, the second term is $D_\ell(m)$ for the vortex, and last two terms correspond to correlations between G and V , which should be statistically negligible after summation over m . If the vortex component is sub-dominant, then in Eq.(6) and Eq.(9) $|V_{\ell m}| \ll |G_{\ell m}|$ for all ℓ, m and $|a_{\ell m}|$ is given by Eq.(6). This means that $|g_{\ell m}| \simeq 1$ and $|v_{\ell m}| \ll 1$. However, because of finite number of m modes and especially for low ℓ range, correlations can manifest themselves between $(\ell-1, m)$, $(\ell+1, m)$ harmonics. In order of magnitude this effect can be estimated by the following way. For pure Gaussian signal with non-correlated phases $\phi_{\ell m}$ one obtains

$$\frac{1}{\ell} \sum_{m=1}^{\ell} \cos \phi_{\ell m} \simeq \frac{1}{\sqrt{\ell}}; \quad \frac{1}{\ell} \sum_{m=1}^{\ell} \sin \phi_{\ell m} \simeq \frac{1}{\sqrt{\ell}}. \quad (10)$$

Then, for the moduli $|a_{\ell m}|$ from Eq.(6) one gets

$$\begin{aligned} |a_{\ell m}|^2 &\simeq |G_{\ell m}|^2 + |V_{\ell m}|^2 \\ \text{if } &|V_{\ell m}| \gg |G_{\ell m}|/\sqrt{\ell}; \\ |a_{\ell m}|^2 &\simeq |G_{\ell m}|^2 + 2|G_{\ell m}||V_{\ell m}| \cos(\Psi_{\ell m}^G - \Psi_{\ell m}^V), \\ \text{if } &|V_{\ell m}| \ll |G_{\ell m}|/\sqrt{\ell}. \end{aligned} \quad (11)$$

For the asymptotic $|V_{\ell m}| \gg |G_{\ell m}|/\sqrt{\ell}$,

$$\begin{aligned} \mathbf{C}(\ell) &\sim \frac{1}{\sqrt{\ell}} - \frac{1}{\ell^{\frac{3}{2}}} \sum_m \frac{|V_{\ell-1,m}| |V_{\ell+1,m}|}{|G_{\ell-1,m}| |G_{\ell+1,m}|} + \\ &\frac{1}{\ell} \sum_m \frac{|V_{\ell-1,m}| |V_{\ell+1,m}|}{|G_{\ell-1,m}| |G_{\ell+1,m}|} \cos(\Psi_{\ell-1,m}^V - \Psi_{\ell+1,m}^V). \end{aligned} \quad (12)$$

For the correlated phases of the vortex component, the last term in Eq.(12) is larger than the second and, if $\Psi_{\ell-1,m}^V \simeq \Psi_{\ell+1,m}^V$, then

$$\mathbf{C}(\ell) \sim \frac{1}{\sqrt{\ell}} + \frac{\overline{D}_\ell}{\overline{G}_\ell^2}, \quad (13)$$

where \overline{G}_ℓ^2 is the power spectrum of the Gaussian tail.

For highly correlated vortex perturbations, therefore, the contribution to the \mathbf{C} function is significant if $\frac{\overline{D}_\ell}{\overline{G}_\ell^2} \sqrt{\ell} \geq$

1. At $\ell = 100$, $\frac{\overline{D}_\ell}{\overline{G}_\ell^2} \geq 0.1$, which is exactly the DKY criterion for estimation of the magnetic field amplitude for different values of the spectral index n . However, if the observable data sets covering the range of multipoles up to the Silk damping scale ℓ_d for the vortex perturbations, $\ell_d \sim 500$ (Durrer, Kahnashvili & Yates 1998), then non-Gaussian features could be detectable for $\frac{\overline{D}_\ell}{\overline{G}_\ell^2} \geq 0.045$. Moreover, one interesting feature comes from power spectral index dependence of the vortex perturbations mentioned above. For $n = -7$, $\overline{D}_\ell \propto \ell^{-4}$, while \overline{G}_ℓ^2 has the same asymptotic ℓ^{-2} as the Λ CDM WMAP best fit model at $5 < \ell < 30$. For that model of the power index, the most stringent constraint should come from statistics of the low multipoles from the WMAP data, then from high multipole range $\ell \sim \ell_d$ and simple estimator could be $6 \div 7$ times bigger than in DKY: $\frac{\overline{D}_\ell}{\overline{G}_\ell^2} \sim 0.6 \div 0.7$.

We would like to point out that the above-mentioned properties of the \mathbf{C} statistics provide natural explanations

in terms of the cosmic variance limit of error bars for any CMB experiments. Assuming no systematic effect present in the data, for low multipoles $\ell < 100$ the cosmic variance limit corresponds to $\delta C_\ell/C_\ell \simeq (f_{\text{sky}}\ell)^{-\frac{1}{2}}$, where f_{sky} is the sky coverage of the observation. The whole sky WMAP coverage gives $f_{\text{sky}} = 1$. If some part of the CMB power spectrum is related to vortex perturbations, then (Chen et al. 2004)

$$C_\ell = \overline{G}_\ell^2 + \overline{C}_\ell \sim \overline{G}_\ell^2 + |n+1| \left[\frac{\Gamma(-\frac{n+1}{2})}{\Gamma(-\frac{n}{2})} \right]^2 \overline{D}_\ell. \quad (14)$$

Using the definition $\delta C_\ell/C_\ell = (C_\ell - \overline{G}_\ell^2)/\overline{G}_\ell^2$, which corresponds to the contribution of the vortex perturbations to the power spectrum, we have the following threshold of detectability

$$|n+1| \left[\frac{\Gamma(-\frac{n+1}{2})}{\Gamma(-\frac{n}{2})} \right]^2 \overline{D}_\ell/\overline{G}_\ell^2 > \frac{1}{\sqrt{\ell}}, \quad (15)$$

which is in perfect agreement with our estimation Eq.(13).

Let us briefly discuss the properties of the \mathbf{S} statistics. Similar to Eq.(9) one can prove that $\sin(\Psi_{\ell-1,m} - \Psi_{\ell+1,m})$ is given by Eq.(9) with transition from cosine to sine function. However, because of sin dependency, if phases of the non-Gaussian tail are highly correlated, we have degradation of the $|v_{\ell-1,m}| |v_{\ell+1,m}| \sin(\Phi_{\ell-1,m}^V - \Phi_{\ell+1,m}^V)$ term, even if $|V_{\ell m}| \gg |G_{\ell m}|/\sqrt{\ell}$. So, if the phases of the vortex perturbations $\Psi_{\ell-1,m}^V - \Psi_{\ell+1,m}^V$ are highly correlated, for the \mathbf{S} statistics we get $\mathbf{S} \sim 1/\sqrt{\ell}$. Thus, the presence of vertex perturbation (as all non-Gaussian signals) in the CMB data manifest itself as asymmetry of the \mathbf{C} - \mathbf{S} statistics, while for the pure Gaussian signals it should be symmetrical one. In order of magnitude this asymmetry for each mode ℓ is

$$A(\ell) = \frac{\mathbf{S}(\ell)}{\mathbf{C}(\ell)} = \frac{1}{1 + \sqrt{\ell} \frac{\overline{D}_\ell}{\overline{G}_\ell^2}} \ll 0.5, \quad (16)$$

for highly correlated phases of vortex perturbations. Addition to Eq.(16) we can define global asymmetry of the signal

$$A_g = \left| \frac{\sum_\ell \mathbf{S}(\ell)}{\sum_\ell \mathbf{C}(\ell)} \right|. \quad (17)$$

In terms of circular statistical variables (Fisher 1993), this global asymmetry corresponds to the mean angle $\Theta = \tan^{-1} A_g$ for orientation of all harmonics (ℓ, m) in the CMB map. Needles to say, for vertex perturbations with $n = -5$ global asymmetry is expected to be in order of magnitude

$$A_g = \frac{1}{1 + \frac{\overline{D}_\ell}{\overline{G}_\ell^2} \ell_{\text{max}}}, \quad (18)$$

and can be detectable, if $\frac{\overline{D}_\ell}{\overline{G}_\ell^2} \ell_{\text{max}} \gg 1$. At the end of this section we would like to mention one peculiar asymptotic of the $A(\ell)$ and A_g parameters related with correlations of phases. From Eq.(12) one can find that correlation $\Psi_{\ell-1,m}^V - \Psi_{\ell+1,m}^V = \pi/2, 3\pi/2$ leads to $A(\ell), A_g > 1$. So any peaks of the function $A(\ell), A_g \gg 1$ are the mark of $\pi/2, 3\pi/2$ correlations for the non-Gaussian tail of the CMB signal. Below in addition to definition Eq.(8) we introduce the phase difference

$$D_{\ell m}(\Delta\ell) = \Psi_{\ell-\frac{\Delta\ell}{2}, m} - \Psi_{\ell+\frac{\Delta\ell}{2}, m} \quad (19)$$

for even $\Delta\ell$ and

$$D_{\ell m}(\Delta\ell) = \Psi_{\ell+\Delta\ell, m} - \Psi_{\ell-\Delta\ell-1, m} \quad (20)$$

for odd $\Delta\ell$ and corresponding circular moments $\mathbf{S}_{\Delta\ell}(\ell)$ and $\mathbf{C}_{\Delta\ell}(\ell)$ similar to Eq.(8). These variables allow us to describe properties of the CMB phases for any $\Delta\ell$ separations of the modes.

3. CIRCULAR STATISTICS OF THE ILC, FCM AND WFCM MAPS DERIVED FROM THE WMAP DATA

In this section we apply the \mathbf{S} , \mathbf{C} statistics for the three high resolution whole-sky maps: the Internal Linear Combination Map (ILC) by the WMAP science team, the TOH foreground-cleaned map (hereafter FCM) and the TOH Wiener-filtered map (hereafter WFCM). The ILC and the FCM are obtained from a weighted combination of the WMAP 5 maps at frequency 23, 33, 41, 61 and 94 GHz in order to separate the microwave foreground. The WFCM is the map after foreground residue cleaning by Wiener filtering. All the maps formally claim resolution up to $\ell = 1024$, but none of them is correct for investigation of the CMB properties. The ILC map, as is mentioned at the WMAP website, is applicable for the foregrounds property investigation at the range of multipoles $\ell < 300$. The FCM and WFCM are smoothed for the multipole range $\ell > 300$ by a Gaussian window function and the CMB signal is completely erased by the smoothing. However, looking at the V and Q bands of the WMAP data and combining all the foregrounds (synchrotron, free-free, dust emission) and the point sources from the WMAP catalog, one can find that this map reproduces the CMB signal outside the Kp2 Galactic cut mask extremely well at the range of multipoles $\ell \leq 50$.

The FCM and WFCM have well-defined scale of smoothing in the image domain. However, smoothing does not change at all the phases of the signal even down to the limit $\ell = 1024$. So, using FCM and WFCM we can examine the phases at the whole range of multipoles. One additional reason for using the FCM and WFCM maps is that they are tested by ESS method, from which the manifestation of the Alfvén turbulence properties could be clearly seen (Bershanskii & Sreenivasan 2003, 2004).

In Fig.1 we plot for the three maps (ILC, FCM and WFCM) the \mathbf{S} - \mathbf{C} phase diagrams for $\Delta\ell = (\ell+1) - (\ell-1) = 2$. For comparison we include the statistics of Gaussian random signal, which reproduce our expectation of the phase properties. From the second row in Fig.1 one can see that ILC phases perfectly reproduce the properties of Gaussian signal phases in terms of $\mathbf{S}(\ell)$, $\mathbf{C}(\ell)$ and $A(\ell)$ variables. One can see that on the third and the fourth row, which corresponds to the FCM and WFCM maps, starting from $\ell \sim 100$ the \mathbf{S} - \mathbf{C} symmetry is broken, and while the \mathbf{S} follows Gaussian statistics, its \mathbf{C} and $A(\ell)$ appear non-Gaussian.

According to Fig.1, the phases of the FCM and WFCM are in agreement with the expectation, described in previous Section. We have significant increase of the \mathbf{C} statistics, while \mathbf{S} statistics are nearly the same as for the Gaussian signal. However, next three Figures display clearly non-Gaussianity. Fig.2 are the circular statistics $\mathbf{S}(\ell)$, $\mathbf{C}(\ell)$ and $A(\ell)$ for $\Delta\ell = 1$, and Fig.4 and Fig.3 are for $\Delta\ell = 3$ and $\Delta\ell = 4$ respectively. According to DKY, for all $\Delta\ell \neq 2$ the phases of the signal should not display any

correlated features. One can also find remarkable symmetry in the FCM and WFCM between even and odd $\Delta\ell$ statistics (e.g. the \mathbf{C} in Fig.1 and Fig.4 and the \mathbf{S} in Fig.2 and Fig.3).

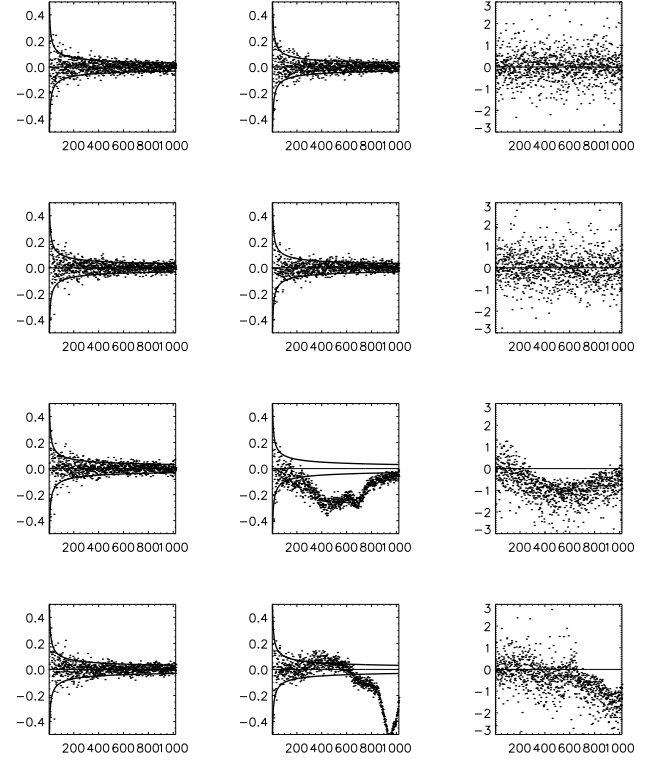


FIG. 1.— Circular statistics on phase correlations with $\Delta\ell = 2$. The columns (from left to the right) correspond to $\mathbf{S}(\ell)$, $\mathbf{C}(\ell)$ and $\log A(\ell)$, respectively. The first row is for a Gaussian realization (random phases). The second row is the ILC map, the third the FCM map and the last the WFCM map.

$$\begin{aligned} \text{sign} \mathbf{C}_{\Delta\ell} &= -\text{sign} \mathbf{C}_2 \cos\left(\frac{\pi}{2}\Delta\ell\right), \text{ for even } \Delta\ell \\ \text{sign} \mathbf{S}_{\Delta\ell} &= \text{sign} \mathbf{S}_1 \sin\left(\frac{\pi}{2}\Delta\ell\right), \text{ for odd } \Delta\ell. \end{aligned} \quad (21)$$

This symmetry reflects the symmetry of the phases $D_{\Delta\ell}(\ell)$, namely

$$\Psi_{\ell+\frac{\Delta\ell}{2}, m} - \Psi_{\ell-\frac{\Delta\ell}{2}, m} = \frac{\pi}{2}\Delta\ell + \pi \quad (22)$$

for even $\Delta\ell$ and

$$\Psi_{\ell+\Delta\ell, m} - \Psi_{\ell-\Delta\ell-1, m} = \frac{\pi}{2}\Delta\ell \quad (23)$$

for odd $\Delta\ell$ and for all values of m .

4. NON-LINEAR STATISTICS

In this section in order to investigate the properties of non-Gaussianity, we apply non-linear statistics $r^2(\ell)$ for the ILC, FCM and WFCM phases. From Eq.(8) one obtains

$$r^2(\ell) = \frac{1}{\ell-1} + \sum_m \sum_{n \neq m} \frac{\cos[D_{\ell m}(\Delta\ell) - D_{\ell n}(\Delta\ell)]}{(\ell-1)^2} \quad (24)$$

That means, that r -statistics are sensitive to m dependence of the phase difference for given values ℓ and $\Delta\ell$.

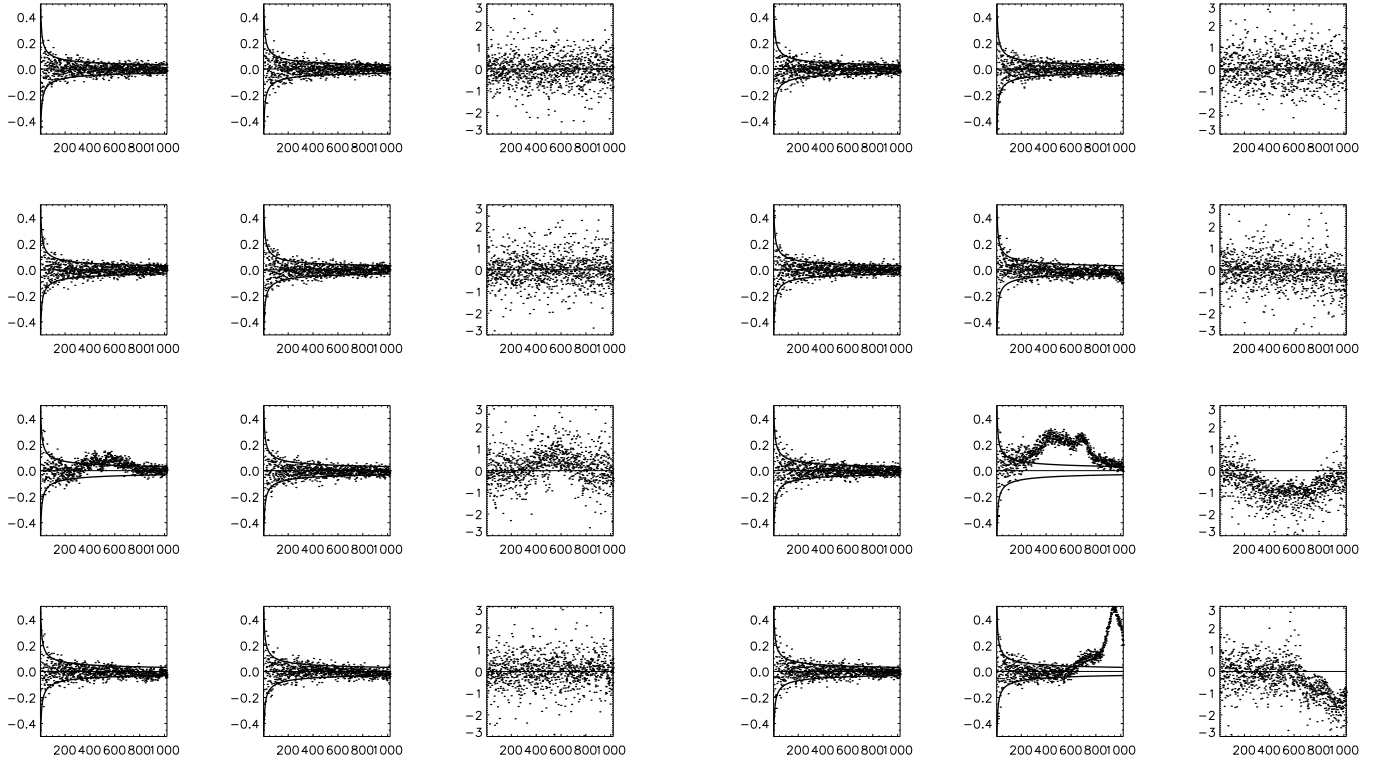


FIG. 2.— The same as in Fig.1, but for $\Delta\ell = 1$.

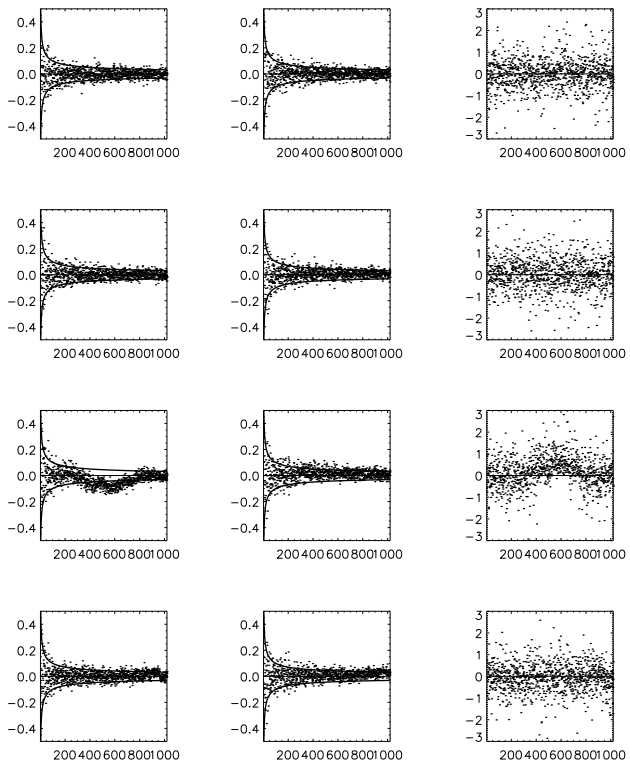


FIG. 3.— The same as in Fig.1, but for $\Delta\ell = 3$.

FIG. 4.— The same as Fig.1, but for $\Delta\ell = 4$.

This statistic has well-defined properties. If the signal is highly correlated and $D_{\ell m}(\Delta\ell) \rightarrow 0$ then $r^2(\ell) \rightarrow 1$. If the phases are non-correlated, however, $r^2(\ell) \rightarrow \ell^{-1}$. In Fig.5 and 6 we plot $r^2(\ell)$ versus ℓ for the same model and the same order as in Fig.1. For all even $\Delta\ell$ the corresponding $r^2(\ell)$ are similar to Fig.5 and for all odd $\Delta\ell$ the r^2 statistics follow Fig.6.

Like **S** and **C** statistics, $r^2(\ell)$ statistics reflect non-Gaussian features for $\Delta\ell = 1, 2, 3, \dots$, which allow us to conclude that non-Gaussianity of FCM and WFCM does not relate with the vortex turbulence at the epoch of recombination. Moreover, in the next Section we will show, how the symmetry of the **S** and **C** statistics allow us to detect the source of non-Gaussianity of FCM and WFCM.

5. LOCAL DEFECTS OF THE ILC, FCM AND WFCM MAPS

In order to detect the nature of the non-Gaussianity of the maps with different powers of signals, we will use the power filter $P(\ell) = 1/|a_{\ell m}|$, proposed by Górski (1997) and Novikov et al. (2001). This linear filter transforms any maps with $a_{\ell m}$ coefficients of spherical harmonic expansions to maps with the same amplitude ($= 1$) at each mode ℓ, m , but preserving all the phases $\Psi_{\ell m}$ and their correlations.

$$N_{\ell m} = P(\ell)a_{\ell m} = \exp(i\Psi_{\ell m}) \quad (25)$$

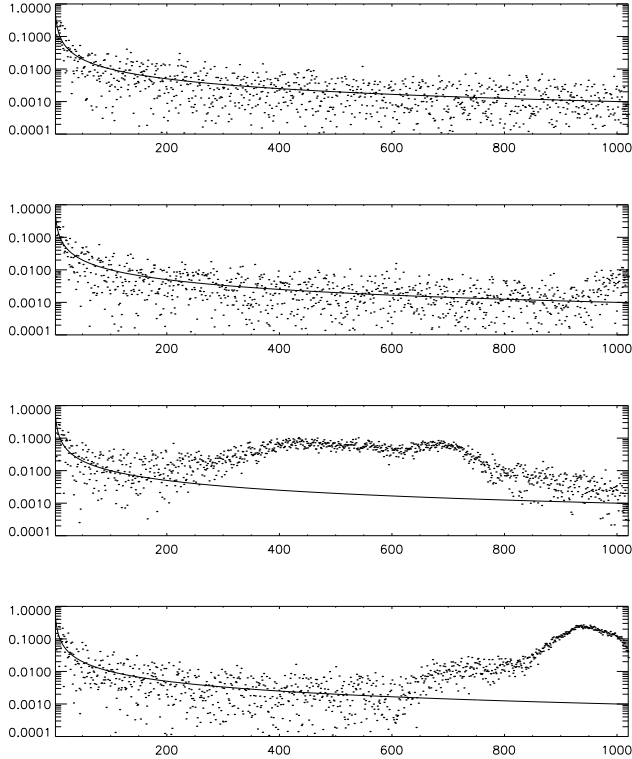


FIG. 5.— $r^2(\ell)$ statistics for $\Delta\ell = 2$ for (from top to bottom) a Gaussian random realization, ILC, FCM and WFCM, respectively. Solid line corresponds to $r^2(\ell) = \ell^{-1}$ asymptotic.

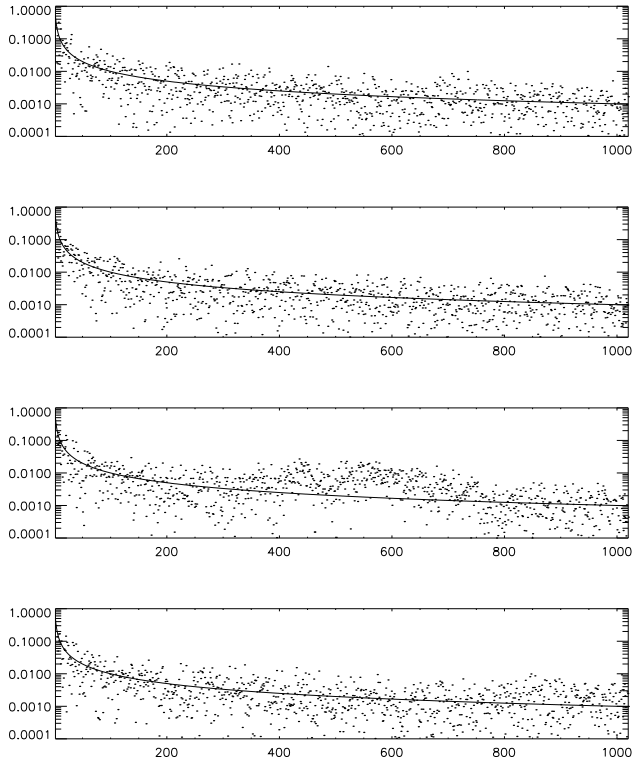


FIG. 6.— The same as in Fig.5, but for $\Delta\ell = 1$.

In Fig.7 we plot the power filtered ILC, FCM and WFCM maps after power filtration for the range of mul-

tipoles up to $\ell = 1024$ in order to show how power filter allows us to detect some of the local defects of the maps close to the Galactic plane. In particular, one can easily see that there are defects in the ILC map which was originally obscured by the amplitudes $|a_{\ell m}|$. The clear cut features is obviously not of astrophysical origin. One crude guess for such peculiar shape in the middle of the ILC map is that the WMAP science team might have used a direct mask at the center of the map where there are pronounced contaminations from foregrounds and then used Wiener filtering, combining with the best-fit power spectrum, to recover the signal in that area. However, the morphology is related to phases (Chiang 2001) and such mask shall alter the morphology, which manifests itself in the phases. On the other hand, one can see foreground residues in both the FCM and WFCM maps. Qualitatively speaking, these are clear signatures of non-Gaussianity.

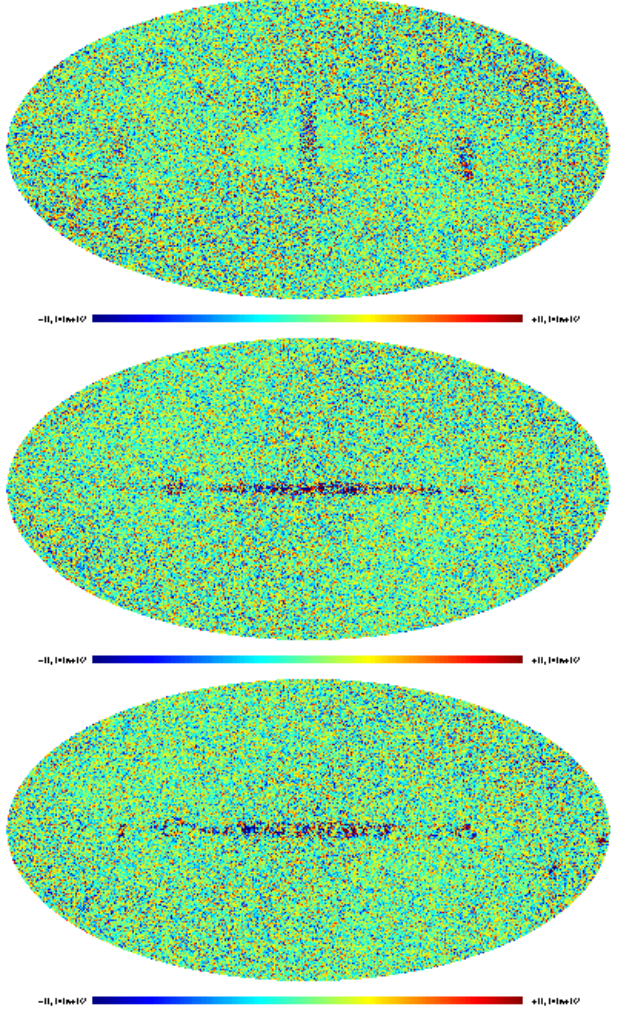


FIG. 7.— The ILC (top), FCM (middle) and WFCM (bottom) power filtered maps. These whiten images are to display how foreground cleaning and the residues manifest themselves in phases, which are otherwise obscured by the amplitudes $|a_{\ell m}|$. One can see the clear cut feature in the middle of the ILC map and galactic and point source contaminations for FCM and WFCM. Qualitatively, these are clear signatures of non-Gaussianity.

Using Eq.(25), one can easily visualize the $N_{\ell-\frac{\Delta\ell}{2},m}N_{\ell+\frac{\Delta\ell}{2},m}$ cros-correlations using simple definition

$$G_{\ell m}(\Delta\ell) = N_{\ell-\frac{\Delta\ell}{2},m}N_{\ell+\frac{\Delta\ell}{2},m}^* = \exp[iD_{\ell m}(\Delta\ell)] \quad (26)$$

For these maps the common features, like a small in

size clusters, seems to be typical (corresponding statistics one can find in Naselsky, Doroshkevich & Verkhodanov (2004)). In order to show how local defects of the maps can produce corresponding features, let us introduce the following model of sub-dominant non-Gaussian signal. Suppose that we have a set of points (pixels) with coordinates θ_j, ϕ_j in which the signal looks like a combination of δ -functions

$$\Delta T_{loc}(\theta, \phi) = \sum_j A_j \delta(\phi - \phi_j) \delta(\cos \theta - \cos \theta_j), \quad (27)$$

where A_j are the amplitudes of defects. In order to obtain the corresponding $c_{\ell m}$ coefficients, we convolve ΔT from Eq.(27) with conjugated spherical harmonics

$$\begin{aligned} c_{\ell m} &= \int_{-1}^1 d(\cos \theta) \int_{-\pi}^{\pi} d\phi \Delta T_{loc}(\theta, \phi) Y_{\ell m}^*(\theta, \phi) \\ &= \sum_i A_i Y_{\ell m}^*(\theta_i, \phi_i) \end{aligned} \quad (28)$$

5.1. Peculiarities of $\Delta\ell$ -even statistics

To obtain the correlators for **S** and **C** statistics, we need to know $\cos[D_{\ell m}(\Delta\ell)]$ and $\sin[D_{\ell m}(\Delta\ell)]$, which can be found from Eq.(28) as

$$\begin{aligned} C_{\ell m}(\Delta\ell) &= |c_{\ell-\frac{\Delta\ell}{2}, m}| |c_{\ell+\frac{\Delta\ell}{2}, m}| \cos [D_{\ell m}(\Delta\ell)] \\ &= \left(c_{\ell-\frac{\Delta\ell}{2}, m} c_{\ell-\frac{\Delta\ell}{2}, m}^* + c_{\ell+\frac{\Delta\ell}{2}, m}^* c_{\ell+\frac{\Delta\ell}{2}, m} \right) / 2 \\ S_{\ell m}(\Delta\ell) &= |c_{\ell-\frac{\Delta\ell}{2}, m}| |c_{\ell+\frac{\Delta\ell}{2}, m}| \sin [D_{\ell m}(\Delta\ell)] \\ &= \left(c_{\ell-\frac{\Delta\ell}{2}, m} c_{\ell-\frac{\Delta\ell}{2}, m}^* - c_{\ell+\frac{\Delta\ell}{2}, m}^* c_{\ell+\frac{\Delta\ell}{2}, m} \right) / 2i \end{aligned} \quad (29)$$

Taking into account Eq.(28), from Eq.(29) we have

$$\begin{aligned} C_{\ell m}(\Delta\ell) &= \sum_{j,k} B_{jk}(\ell, m) \cos [m(\phi_j - \phi_k)] \\ &\quad \times P_{\ell-\frac{\Delta\ell}{2}}^m(\cos \theta_j) P_{\ell+\frac{\Delta\ell}{2}}^m(\cos \theta_k) \\ S_{\ell m}(\Delta\ell) &= \sum_{j,k} B_{jk}(\ell, m) \sin [m(\phi_j - \phi_k)] \\ &\quad \times P_{\ell-\frac{\Delta\ell}{2}}^m(\cos \theta_j) P_{\ell+\frac{\Delta\ell}{2}}^m(\cos \theta_k) \end{aligned} \quad (30)$$

where $P_{\ell}^m(\cos \theta)$ are the associated Legendre polynomials and

$$\begin{aligned} B_{jk}(\ell, m) &= \\ A_j A_k \left[\frac{\Gamma(\ell - \frac{\Delta\ell}{2} - m + 1) \Gamma(\ell + \frac{\Delta\ell}{2} - m + 1)}{\Gamma(\ell - \frac{\Delta\ell}{2} + m + 1) \Gamma(\ell + \frac{\Delta\ell}{2} + m + 1)} \right]^{\frac{1}{2}} \end{aligned} \quad (31)$$

Following Naselsky, Doroshkevich & Verkhodanov (2003), let us describe an ideal situation when $\theta_j = \theta_k = \pi/2$, but $\phi_j \neq \phi_k$. For this model in Eq.(30) we get

$$\begin{aligned} P_{\ell-\frac{\Delta\ell}{2}}^m(0) &= \\ \sqrt{\pi} 2^m \left[\Gamma \left(1 + \frac{\ell - m - \frac{\Delta\ell}{2}}{2} \right) \Gamma \left(\frac{1 - \ell - m + \frac{\Delta\ell}{2}}{2} \right) \right]^{-1} \end{aligned} \quad (32)$$

As one can see from Eq.(32) and Eq.(30) the major part of the summation over m is related with $m = \ell - \frac{\Delta\ell}{2}$, for

which

$$\begin{aligned} P_{\ell-\frac{\Delta\ell}{2}}^m(0) P_{\ell+\frac{\Delta\ell}{2}}^m(0) |_{m=\ell-\frac{\Delta\ell}{2}} &= \\ 2^{2\ell-\Delta\ell} \pi \frac{\Gamma(\frac{1}{2} + (\ell - \frac{\Delta\ell}{2})) \Gamma(\frac{1}{2} + \ell)}{\Gamma(\frac{1}{2} + \frac{\Delta\ell}{2})} \cos(\frac{\pi \Delta\ell}{2}) \end{aligned} \quad (33)$$

Thus, the sign of the $C_{\ell m}(\Delta\ell)$ for even $\Delta\ell$ is determined by the cosine terms. Moreover, if $\Delta\ell = 2n$, $n = 1, 2, 3 \dots$, the contribution of the local defects with $\theta_j = \pi/2$ to **C** statistics manifest itself as the changes of the sign, mentioned in Eq.(21). One may ask, why are **S** and **C** statistics so different, if they depends on θ_j in the same way? Taking into account the ϕ_j dependency of $C_{\ell m}(\Delta\ell)$ and $S_{\ell m}(\Delta\ell)$ one can see that for $j = k$ the cosine terms in Eq.(30) ($\cos[m(\phi_j - \phi_k)]$) goes to unity while the sine terms for $S_{\ell m}(\Delta\ell)$ is equal to zero. All $j \neq k$ modes in Eq.(30) are represented by highly oscillated functions and look like a noise in the phase diagrams (see Fig.1-4).

5.2. Peculiarities of odd $\Delta\ell$ statistics

Let us discuss the model $\Delta\ell = 2n + 1$, $n = 1, 2, 3 \dots$. There are two possibilities to understand the properties of the phase correlations for odd $\Delta\ell$. Firstly we discuss the Galactic plane sources contamination. In such a case similar to Eq.(33) one can find

$$P_{\ell-\Delta\ell}^m(0) P_{\ell}^m(0) |_{m=\ell-\Delta\ell} \sim \cos \left(\frac{\pi \Delta\ell}{2} \right), \quad (34)$$

and odd $\Delta\ell$ does not contribute to **S** and **C** statistics, if $\theta_j = \pi/2$ for all j . However, if for some of the local defects $\theta_j \neq \pi/2$, but $\cos \theta_j \ll 1$, there should produce significant peculiarities in **S** statistics by the following way. Close to the Galactic plane we can expand the Legendre polynomials using a Taylor series

$$\begin{aligned} P_{\ell-\Delta\ell}^m(\cos \theta_j) &= P_{\ell-\Delta\ell}^m(0) + \frac{dP_{\ell-\Delta\ell}^m(\cos \theta_j)}{d(\cos \theta_j)}|_{\cos \theta_j=0} \cos \theta_j \\ &\quad + \frac{1}{2} \frac{d^2 P_{\ell-\Delta\ell}^m(\cos \theta_j)}{d(\cos \theta_j)^2}|_{\cos \theta_j=0} \cos^2 \theta_j \end{aligned} \quad (35)$$

Simple algebra allows us to conclude that the dependence $S_{\ell m}(\Delta\ell), C_{\ell m}(\Delta\ell) \propto \cos^2 \theta_j \sin(\pi \Delta\ell/2)$ comes from interference between the first and the last terms in Eq.(35), after their substitution to Eq.(30). Thus, this dependency over $\Delta\ell$ takes place for some of the multipoles, for which $\ell \theta_j \ll 1$, while for $\ell \theta_j \gg 1$ $S_{\ell m}(\Delta\ell), C_{\ell m}(\Delta\ell)$ statistics goes to zero for odd $\Delta\ell$. This dependency of the **S** and **C** statistics over $\Delta\ell$ can be clearly seen in Fig.2 and Fig.3, where symmetry **S** and **C** statistics are restored for high ℓ . However, **S** and **C** statistics as $C_{\ell m}(\Delta\ell)$ depends on $\Delta\ell$ in the same way, while in Fig.2 and Fig.3 one can see significant asymmetry in the **S** and **C** statistics. The reason for that could be localization of the the defects in ϕ direction close to the Galactic center with the width $-\pi/2 \ll \delta \phi_j \ll \pi/2$ in the Galactic coordinates.

6. CONCLUSION

In this paper we examine the primordial non-Gaussian feature from Alvan turbulence caused by primordial magnetic field. The distortion of the blackbody CMB spectrum by such homogeneous magnetic field is not discussed in this paper. Due to the vector nature of the magnetic

field, off-diagonal correlations between spherical harmonic modes $a_{\ell-1,m}$ and $a_{\ell+1,m}$ are induced. To see the $\Delta\ell = 2$ correlations, we apply circular statistics of phases to analyze such non-Gaussian component from the CMB signal. We have applied the statistics on the ILC, FCM and WFCM maps, using all the available phases. The phase information can help us to test some of the properties of the signal even when the amplitude of the power spectra were smoothed by Gaussian window functions starting from $\ell \sim 50 - 200$.

The FCM and WFCM maps have non-Gaussian signature registered in the phases, as we have found phase correlations not only $\Delta\ell = 2$, but also $\Delta\ell = 1, 3$ and 4 . Such strong correlations are related to the residues from component separation in the Galactic plane and some point sources. None of the maps shows specific features from the vortex perturbations at the last scattering surface. Moreover, the detected non-Gaussianity is completely different from the vortex perturbations properties. Roughly speaking, all the modes with $\Delta\ell = 1, 2, 3$ and 4 show pronounced correlations, which is not the specific features for

the vortex. The correlations such as $\Delta\ell = 4, 8 \dots$ might have been the higher order correlation from $\Delta\ell = 2$, but the $\Delta\ell = 1$ and others indicate that such strong correlations are related to the residues from foreground component separation. We conclude that the Alfvén turbulence does not contribute significantly in the phase information. The method we propose for phase analysis is useful for the upcoming PLANCK mission, especially for testing the properties of foreground cleaning methods. Our final remark is that the MHD structure claimed by Bershadskii (2003) and Bershadskii & Sreenivasan (2004) in the WFCM map is related with Galactic plane residues but not with the Alfvén turbulence contamination.

We thank Tegmark et al. for providing their processed maps. We acknowledge the use of HEALPIX³ package (Górski, Hivon & Wandelt 1999) to produce $a_{\ell m}$ from the WMAP data and the use of the GLESP package (Doroshkevich et al. 2003) for data analyses and the whole-sky figures.

REFERENCES

Bardeen, J. M., Bond, J. R., Kaiser, N., Szalay, A. S., 1986, ApJ, 304, 15
 Bennett, C. L., et al., 2003, ApJ, 583, 1
 Bennett, C. L., et al., 2003, ApJS, 148, 1
 Bennett, C. L., et al., 2003, ApJS, 148, 97
 Bershadskii, A., 2003, Int. J. Mod. Phys. D, 12, 509
 Bershadskii, A., Sreenivasan, K. R., 2003, Phys. Lett. A, 319, 21
 Bershadskii, A., Sreenivasan, K. R., 2004, Int. J. Mod. Phys. D, 13, 281
 Bond, J. R., Efstathiou, G., 1987, MNRAS, 226, 655
 Branderburg, A., Enqvist, K., Olesen, P., 1996, Phys. Rev. D, 54, 1291
 Chen, G., Mukherjee, P., Kahnashvili, T., Ratra, B., Wang, Y., 2004, ApJ in press (astro-ph/0403695)
 Chiang, L.-Y., 2001, MNRAS, 325, 405
 Chiang, L.-Y., Coles, P., 2000, MNRAS, 311, 809
 Chiang, L.-Y., Coles, P., Naselsky, P. D., 2002, MNRAS, 337, 488
 Chiang, L.-Y., Naselsky, P. D., Coles, P., 2004, ApJL, 602, 1
 Chiang, L.-Y., Naselsky, P. D., Verkhodanov, O. V., Way, M. J., 2003, ApJL, 590, 65
 Coles, P., Dineen, P., Earl, J., Wright, D., 2004, MNRAS accepted (astro-ph/0310252)
 de Oliveira-Costa, A., Tegmark, M., Zaldarriaga, M., Hamilton, A., 2004, Phys. Rev. D, 69, 063516
 Doroshkevich, A. G., Naselsky, P. D., Verkhodanov, O. V., Novikov, D. I., Turchaninov, V. I., Novikov, I. D., Christensen, P. R., 2003, A&A submitted (astro-ph/0305537)
 Durrer, R., Kahnashvili, T. A., Yates, A., 1998, Phys. Rev. D, 58, 123004
 Fisher, R., 1993, Statistical Analysis of Circular Data, Cambridge University Press, Cambridge
 Efstathiou, G., 2003, MNRAS, 346, L26
 Eriksen, H. K., Hansen, F. K., Banday, A. J., Górska, K. M., Lilje, P. B., 2004, ApJ, 605, 14
 Eriksen, H. K., Banday, A. J., Górska, K. M., Lilje, P. B., 2004, ApJ submitted (astro-ph/0403098)
 Górski, K. M., 1997, Bouchet F. R. et al. eds., in Proceedings of the XVI Recontres de Moriond, Microwave Background Anisotropies, Edition Frontieres
 Górski, K. M., Hivon, E., Wandelt, B. D., 1999, Banday, A. J., Sheth, R. S. and Da Costa, L. eds., in Proceedings of the MPA/ESO Cosmology Conference "Evolution of Large-Scale Structure", Print Partners Ipskamp, NL
 Hansen, F. K., Cabella, P., Marinucci, D., Vittorio, N., 2004, ApJL in press (astro-ph/0402396)
 Hinshaw, G., et al., 2003, ApJS, 148, 63
 Hinshaw, G., et al., 2003, ApJS, 148, 135
 Komatsu, E., et al., 2003, ApJS, 148, 119
 Larson, D. L., Wandelt, B. D., 2004, ApJL submitted (astro-ph/0404037)
 Mack, A., Kahnashvili, T., Kosowsky, A., 2002, Phys. Rev. D, 65, 123004
 Martinez-Gonzalez, E., Diego, J. M., Vielva, P., Silk, J., 2003, MNRAS, 345, 1101
 Naselsky, P. D., Doroshkevich, A. G., Verkhodanov, O. V., 2003, ApJL, 599, 53
 Naselsky, P. D., Doroshkevich, A. G., Verkhodanov, O. V., 2004, MNRAS, 349, 695
 Naselsky, P. D., Novikov, D. I., Silk, J., 2002, ApJ, 655, 565
 Novikov, D., Naselsky, P., Jorgensen, H. E., Christensen, P. R., Novikov, I., Norgaard-Nielsen, H. U., 2001, Int. J. Mod. Phys. D, 10, 245
 astro-ph/0001432
 Park, C.-G., 2004, MNRAS, 349, 313
 Subramanian, K., Seshadri, T. R., Barrow, J. D., 2003, MNRAS, 344, L31
 Scherrer, R. J., Melott, A. L., Shandarin, S. F., 1991, ApJ, 377, 29
 Tegmark, M., Efstathiou, G., 1996, MNRAS, 281, 1297
 Tegmark, M., de Oliveira-Costa, A., Hamilton, A., 2003, Phys. Rev. D accepted (astro-ph/0302496)
 Vielva, P., Martinez-Gonzalez, E., Barreiro, R. B., Sanz, J. L., Cayon, L., 2004, ApJ submitted (astro-ph/0310273)

³ <http://www.eso.org/science/healpix/>